SUPPLEMENTARY INFORMATION

doi:10.1038/nature11726

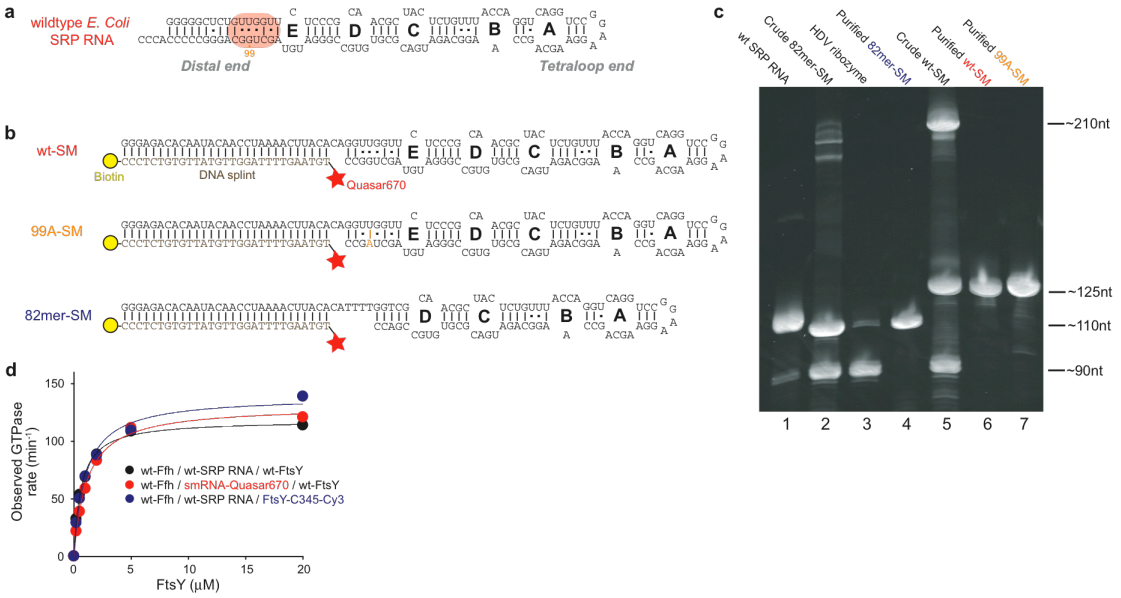

Supplementary Figure 1 | SRP RNA constructs used in single molecule experiments. **a**, Secondary structure of wildtype *E. coli* SRP RNA, which forms an elongated hairpin structure capped by a conserved GGAA tetraloop. Pink region highlights the distal docking site for the SRP-FtsY GTPase complex observed in the crystal structure (PBD code: 2xxa, from Ataide et al, Science, 2011). **b**, Wildtype, 99A, and 82mer smRNA constructs used in this work. **c**, Analytical RNA gel verified the generation and purification of smRNA. smRNAs (lanes 4, 6, 7) were purified from *in vitro* transcription mixtures (lanes 2, 5) by a preparative RNA gel, which removed the HDV ribozyme (90 nt, lane 3) and uncleaved precursor (210 ntd, lane 5). **d**, GTPase reactions for SRPs assembled with DNA-smRNA hybrid and with labeled FtsY.

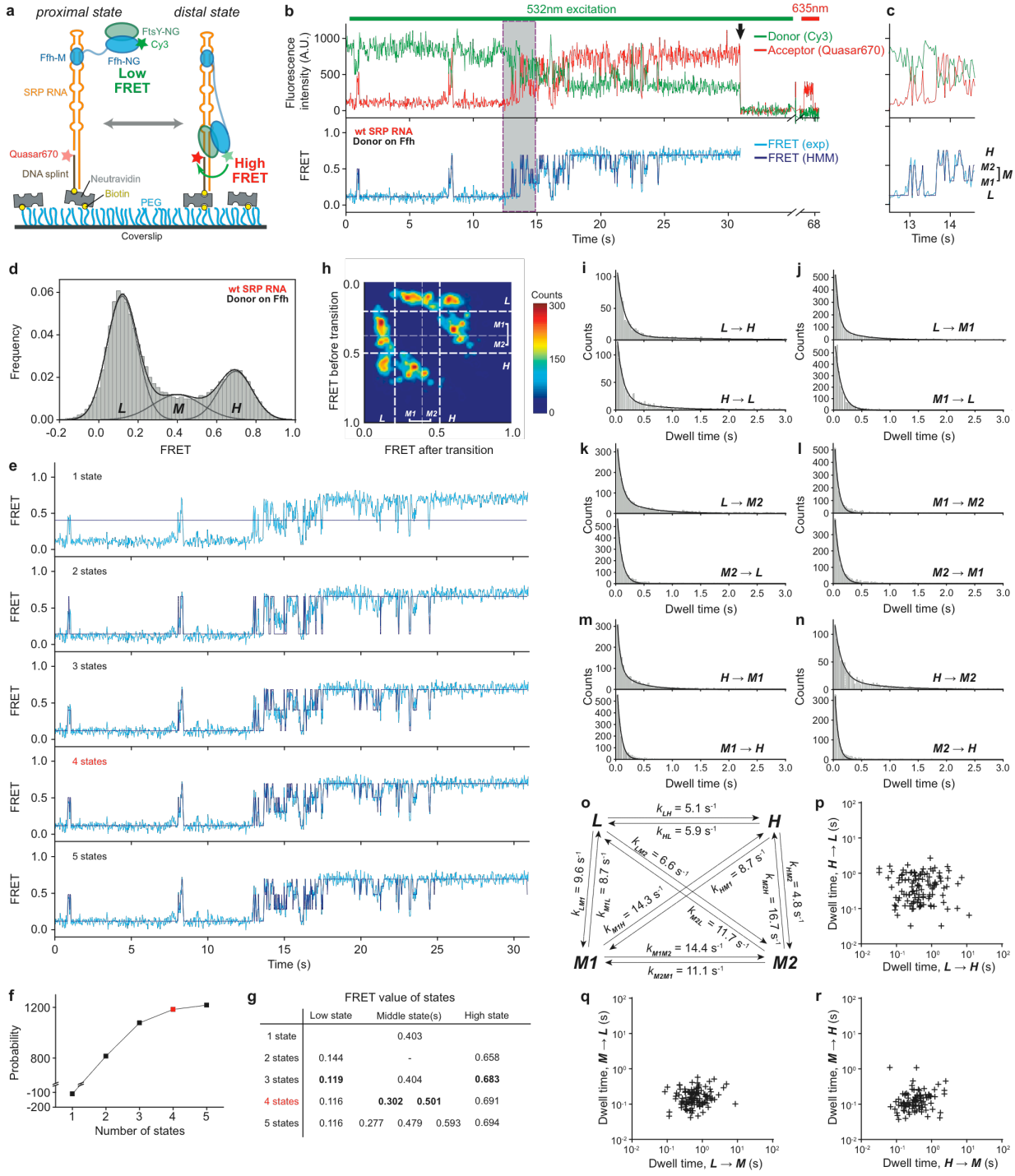

FRET value of states	Low state	Middle state(s)		High state
1 state		0.403		
2 states	0.144	-		0.658
3 states	**0.119**	0.404		**0.683**
4 states	0.116	**0.302**	**0.501**	0.691
5 states	0.116	0.277	0.479	0.593	0.694

Supplementary Figure 2 | smFRET of the SRP-FtsY complex with Cy3-labeled Ffh. **a**, Schematics of the immobilized SRP-FtsY complex on the coverslip with Cy3-labeled Ffh. **b**, Fluorescent signals (upper) and FRET trajectory (lower) of the SRP-FtsY complex. Color coding is the same as in Figure 1b. The arrow denotes bleaching of Cy3. **c**, Zoom in of the grey box in **b** to show the four FRET states resolved by HMM. **d**, smFRET histogram. **e**, HMM analysis of a sample FRET trajectory using different numbers of states. As the number of FRET states increases, better fits to experimental data were obtained. **f**, Probability score of each model in the HMM analysis in **e**. The probability maxed out at 4 states, which was chosen as the optimal model to describe experimental

data. **g**, The FRET values of each state from the HMM analyses in **e**. Bold indicates the converged FRET values of the identified states. **h**, TDP of the GTPase rearrangement. **i-n**, Analysis of the transition kinetics between states ***L*** and ***H*** (**i**), ***L*** and ***M1*** (**j**), ***L*** and ***M2*** (**k**), ***M1*** and ***M2*** (**l**), ***H*** and ***M1*** (**m**), ***H*** and ***M2*** (**n**). **o**, Summary of transition rates between different FRET states. **p-r**, Scatter plots of the transition dwell times of individual molecules. Each cross represents an individual molecule.

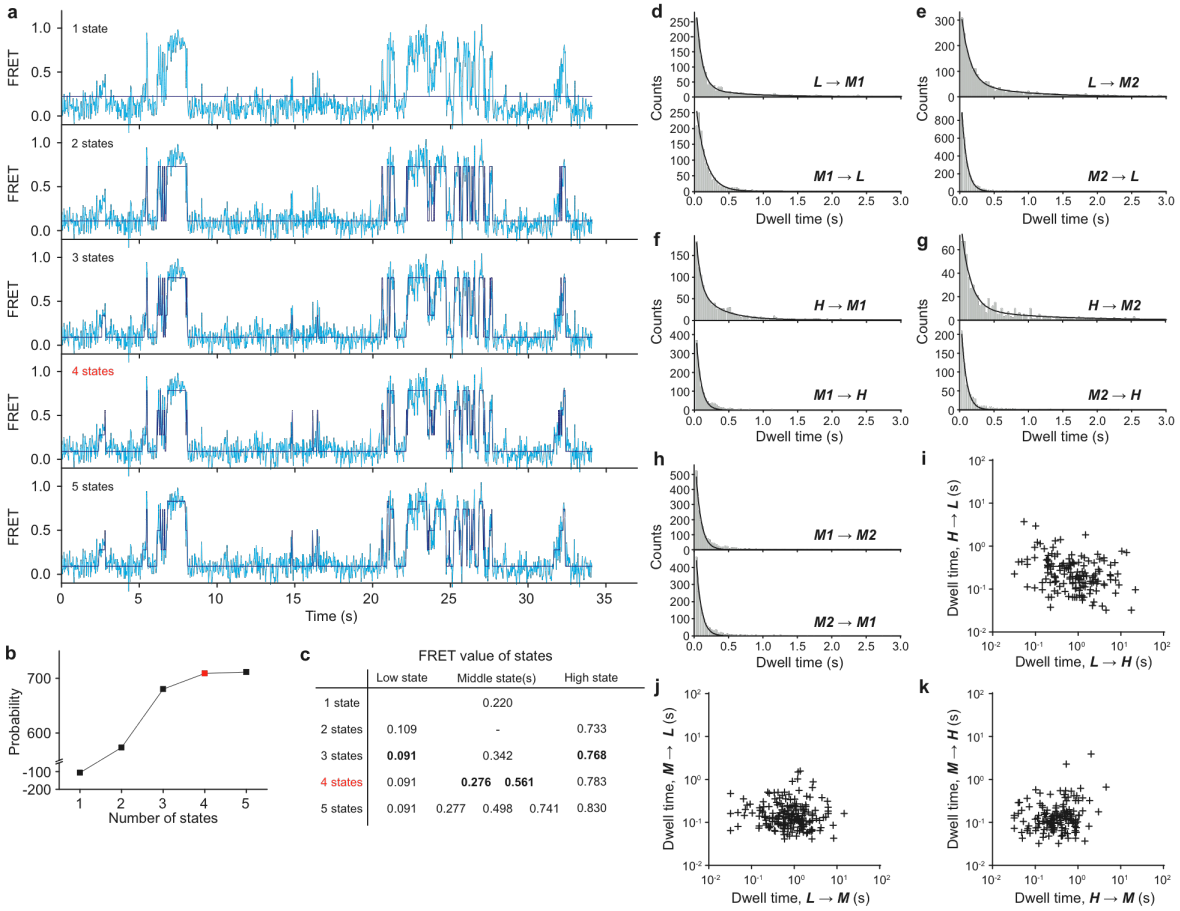

Supplementary Figure 3 | smFRET analysis of the SRP-FtsY complex with labeled FtsY. **a**, HMM analysis of the FRET trajectory in Figure 1b using different numbers of FRET states. As the number of FRET states increases, better fits to experimental data were obtained. **b**, Probability score of each model in the HMM analysis in **a**. The probability maxed out at 4 states, which was chosen as the optimal model to describe experimental data. **c**, The FRET values of each state from the HMM analyses in **a**. Bold indicates the converged FRET values of the identified states. **d-h**, Analysis of the transition kinetics between states ***L*** and ***M1*** (**d**), ***L*** and ***M2*** (**e**), ***H*** and ***M1*** (**f**), ***H*** and ***M2*** (**g**), ***M1*** and ***M2*** (**h**). **i-k**, Scatter plots of the transition dwell times of individual molecules. Each cross represents an individual molecule.

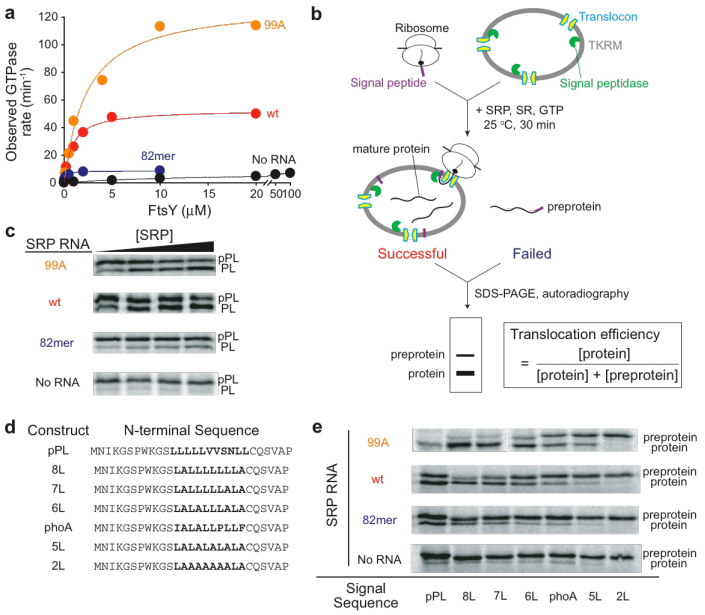

Supplementary Figure 4 | Activity of SRP RNA distal end mutants in GTPase reactions and in co-translational protein targeting and translocation. **a**, Representative data for stimulated GTPase reactions upon assembly of the SRP-FtsY complex with wildtype (red), 82mer (blue), and 99A (orange) SRP RNA. The data in the absence of SRP RNA are in black. Summary of the rate constants, with n = 5, is provided in Figure 2a. **b**, Schematics of the co-translational protein targeting and translocation assay. **c & e,** Representative data for co-translational targeting and translocation of pPL (**c**) and pPL signal sequence variants (**e**) by the wildtype and mutant SRPs. Color coding is the same as in **a**. Quantification of the data from three independent experiments is provided in Figures 2b and c. **d**, Signal sequence variants of pPL used in this study. Bold highlights the hydrophobic core of the signal sequence.

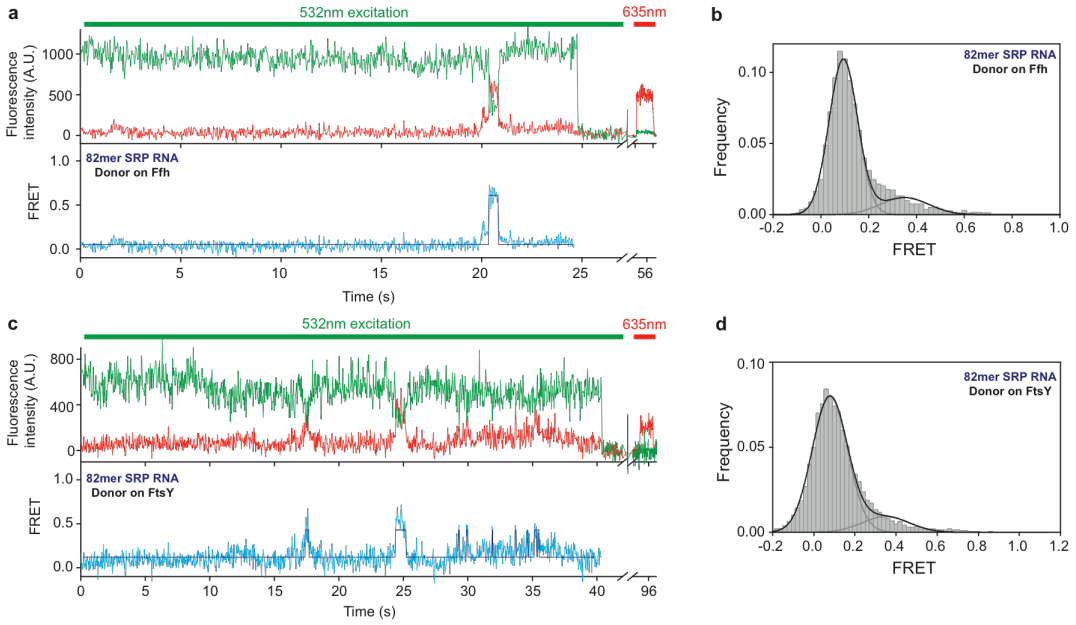

Supplementary Figure 5 | smFRET data and analysis for SRP-FtsY complexes assembled with the 82mer SRP RNA. **a & c**, Fluorescent signals (upper) and FRET trajectory (lower) of the SRP(82mer)-FtsY complex with Cy3-labeled Ffh (**a**) or FtsY (**c**). Color coding is the same as in Figure 1b. **b & d**, smFRET histograms of the GTPase complex with Cy3-labeled Ffh (**b**) or FtsY (**d**).

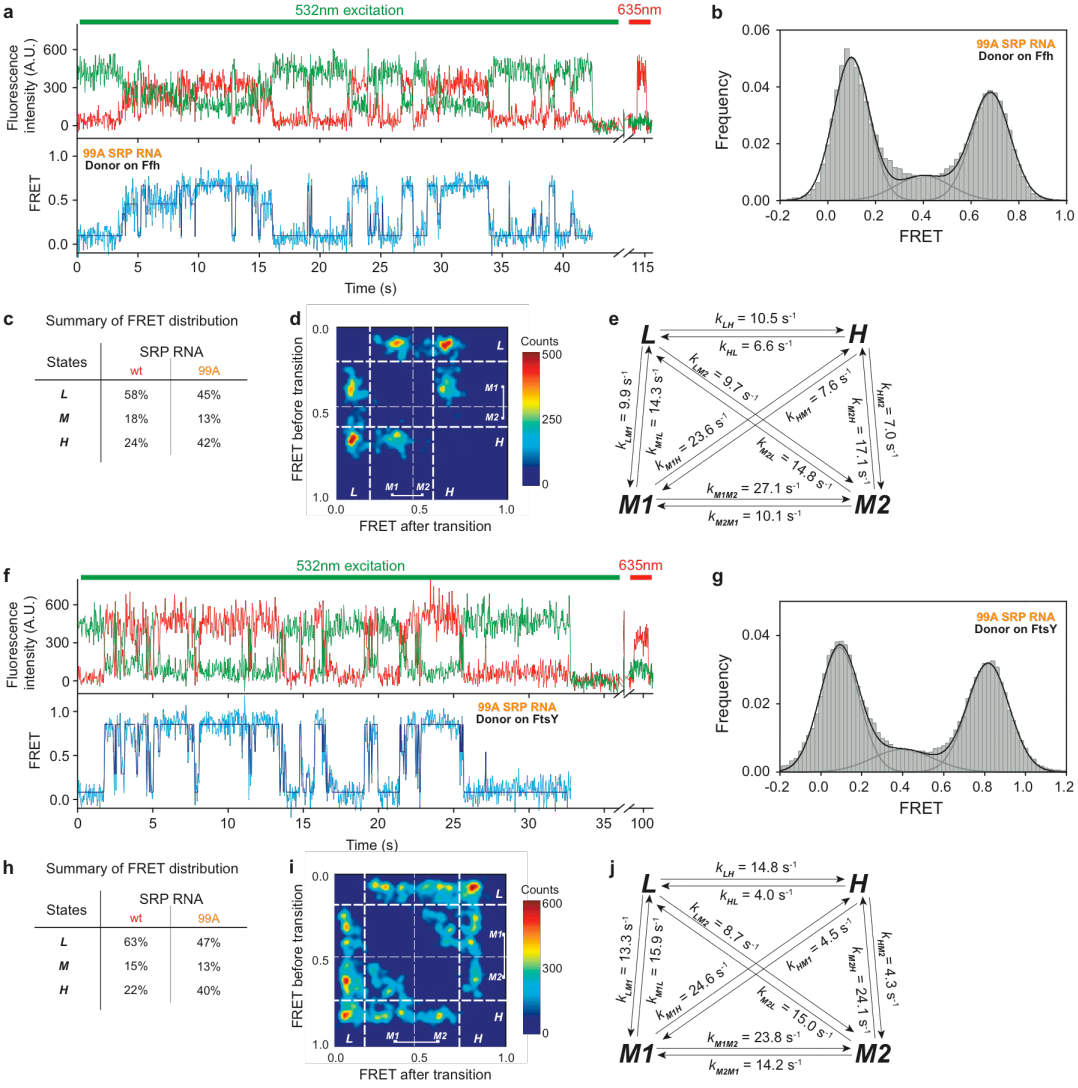

Supplementary Figure 6 | smFRET data and analyses for complexes assembled with mutant 99A RNA. **a & f**, Fluorescent signals (upper) and FRET trajectory (lower) of the SRP(99A)-FtsY complex with Cy3-labeled Ffh (**a**) or FtsY (**f**). Color coding is the same as in Figure 1b. **b & g**, smFRET histograms of the GTPase complex with Cy3-labeled Ffh (**b**) or FtsY (**g**). **c & h**, Summary of the FRET distributions of SRP(99A)-FtsY and comparison with the wildtype complex for Cy3-labeled Ffh (**c**) or FtsY (**h**). **d & i**, TDP of the SRP(99A)-FtsY complex with Cy3-labeled Ffh (**d**) or FtsY (**i**). **e & j**, Summary of transition kinetics of the SRP(99A)-FtsY complex with Cy3-labeled Ffh (**e**) or FtsY (**j**).

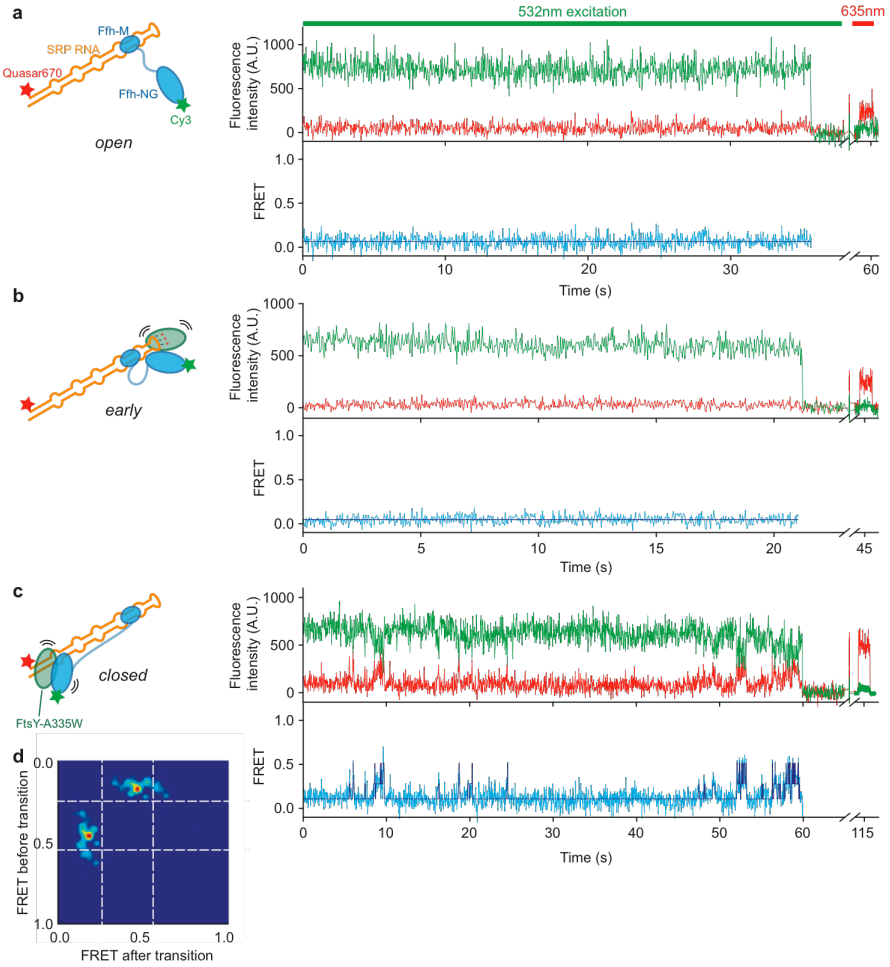

Supplementary Figure 7 | smFRET traces of SRP at different stages of its GTPase cycle, including free SRP (**a**) and the SRP-FtsY complex in the *early* (**b**) and *closed* (**c**) states. Ffh was labeled with Cy3. Color coding is the same as in Figure 1b. **d**, TDP of the SRP-FtsY complex in the *closed* state.

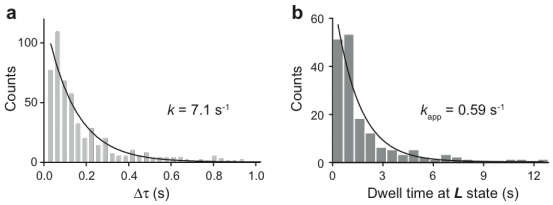

Supplementary Figure 8 | Dwell time analysis of real-time GTP hydrolysis. **a**, Exponential fit of Δτ gave a lower limit for the GTPase rate. **b**, Exponential fit of the low FRET state between high FRET burst clusters.

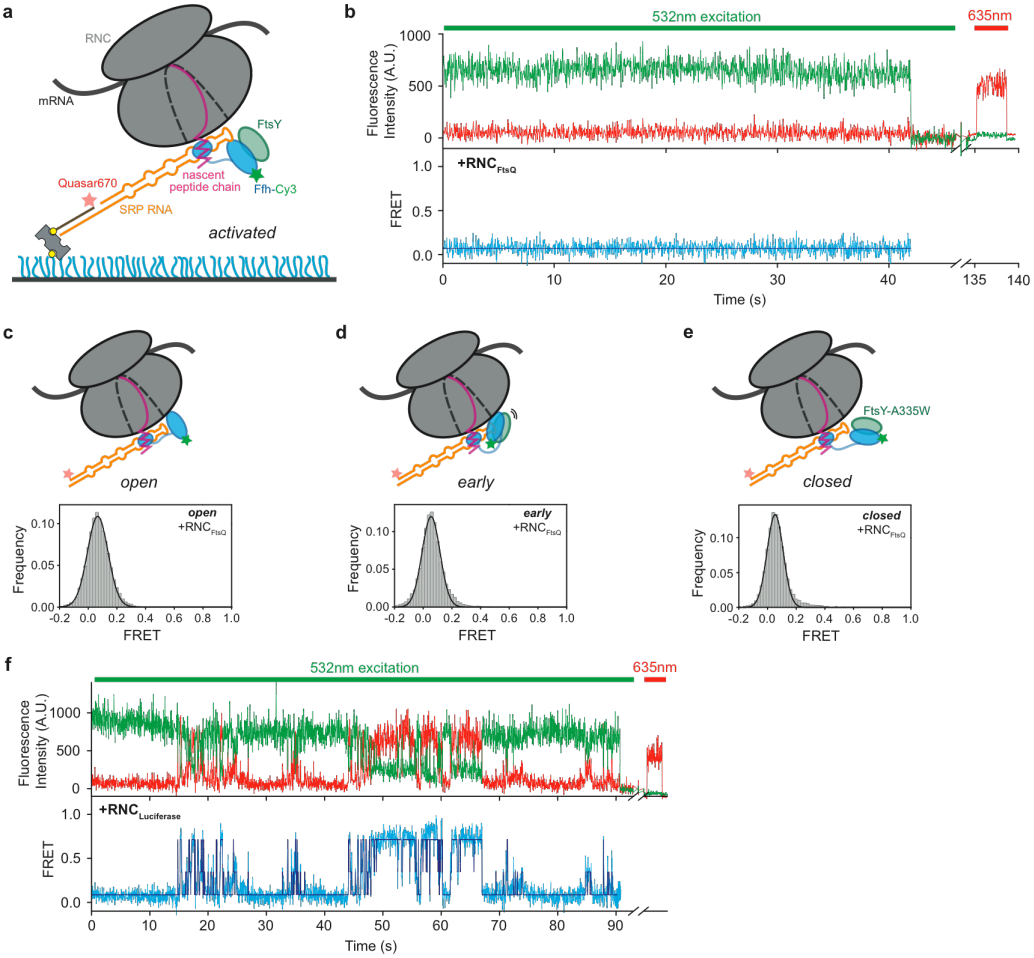

Supplementary Figure 9 | RNC carrying a correct SRP substrate abolishes GTPase movement along the SRP RNA. **a**, RNC-bound SRP-FtsY complex on the coverslip surface. **b & f**, Fluorescent signals (upper) and FRET trajectory (lower) of the SRP-FtsY complex bound to RNC_{FtsQ} (**b**) or $RNC_{luciferase}$ (**f**). Color coding is the same as in Figure 1b. **c-e**, smFRET histograms of the RNC_{FtsQ}-SRP complex (**c**) and the RNC_{FtsQ}-SRP-FtsY complex in the *early* (**d**) and *closed* (**e**) states.

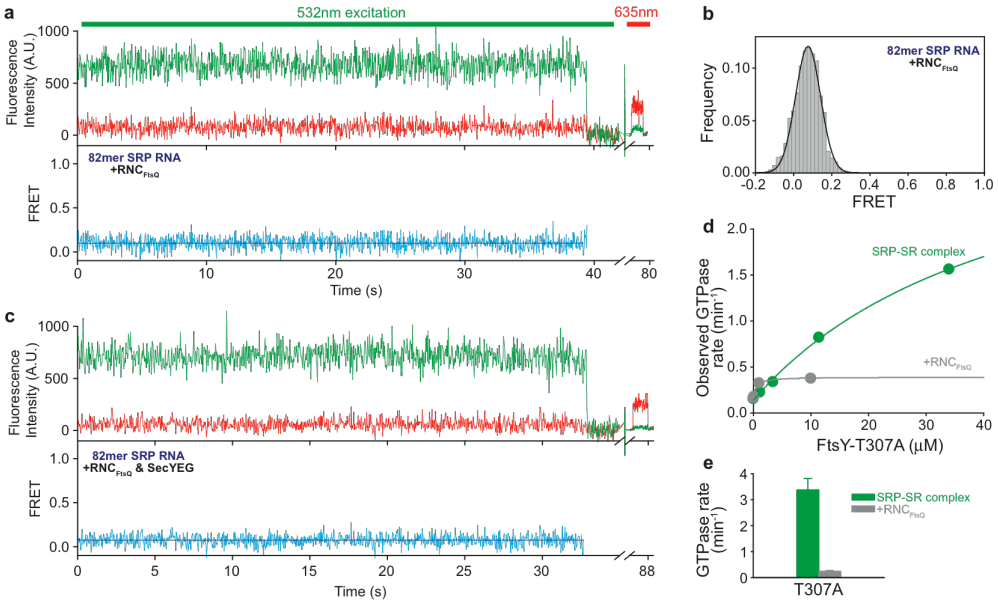

Supplementary Figure 10 | RNC's pausing effect is independent of the SRP RNA distal end. **a & c**, Fluorescent (upper) and FRET (lower) trajectory of the RNC_{FtsQ}-SRP(82mer)-FtsY complex in the absence (**a**) and presence (**c**) of SecYEG. Color coding is the same as in Fig. 1b. **b**, smFRET histogram of the RNC_{FtsQ}-SRP(82mer)-FtsY complex. **d**, Representative data for GTPase assay of mutant FtsY T307A in the absence (green) and presence (grey) of RNC_{FtsQ}. **e**, Summary of the k_{cat} values from (**d**). Data represent mean±s.d. (n=3).

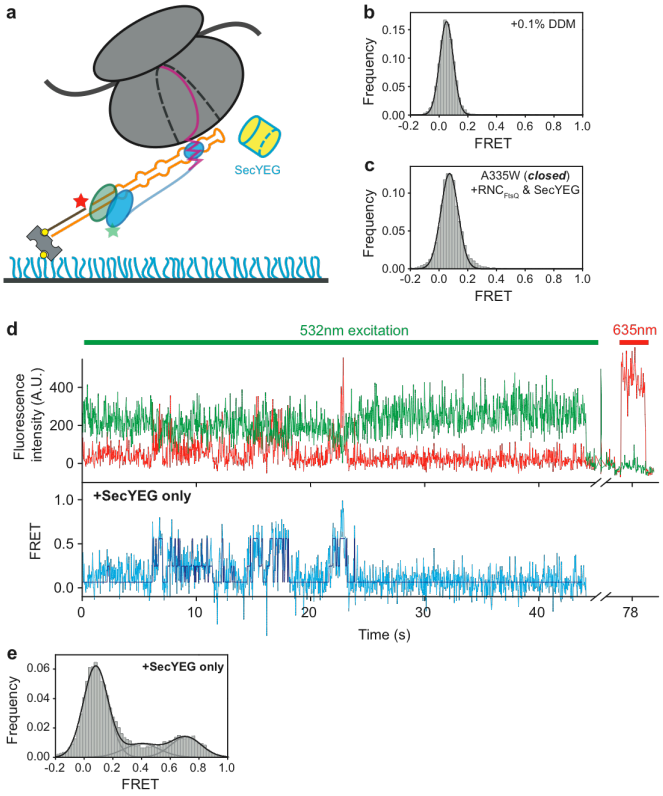

Supplementary Figure 11 | SecYEG restores GTPase movement to the SRP RNA distal site. **a**, SecYEG-bound RNC_{FtsQ}-SRP-FtsY complex on the surface of the coverslip. **b**, smFRET histogram of the RNC_{FtsQ}-SRP-FtsY complex in the presence of 0.1% DDM. For comparison, the DDM concentration in reactions containing SecYEG is ≤0.07%. **c**, smFRET histogram of the RNC_{FtsQ}-SRP-FtsY(A335W) *closed* complex in the presence of SecYEG. **d & e,** FRET trajectory (**d**) and smFRET histogram (**e**) of the SRP-FtsY complex in the presence of SecYEG but absence of RNC. Cy3-labeled Ffh was used.

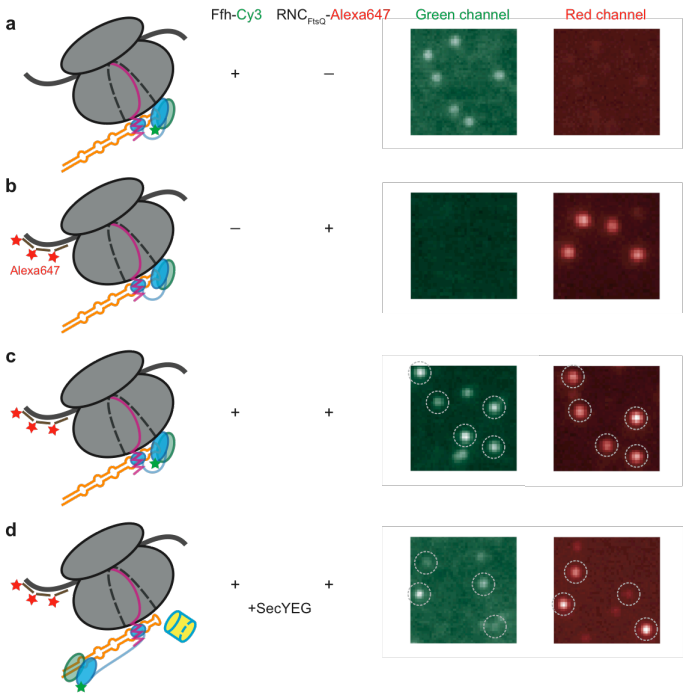

Supplementary Figure 12 | Co-localization assay of SRP and RNC. Cy3-labeled SRP (**a**) and Alexa647-labeled RNC$_{FtsQ}$ (**b**) co-localize before (**c**) and after (**d**) incubation with SecYEG.